



Surface zooplankton size and taxonomic composition in Bowdoin Fjord, north-western Greenland: A comparison of ZooScan, OPC and microscopic analyses



Akihiro Naito^{a,1}, Yoshiyuki Abe^{a,b}, Kohei Matsuno^{a,b}, Bungo Nishizawa^{a,b}, Naoya Kanna^{b,c}, Shin Sugiyama^{b,c}, Atsushi Yamaguchi^{a,b,d,*}

^a Graduate School of Fisheries Science, Hokkaido University, 3-1-1 Minato-cho, Hakodate, Hokkaido, 041-8611, Japan

^b Arctic Research Centre, Hokkaido University, Kita-21 Nishi-11 Kita-ku, Sapporo, Hokkaido, 001-0021, Japan

^c Institute of Low Temperature Science, Hokkaido University, Kita-19 Nishi-8 Kita-ku, Sapporo, Hokkaido, 060-0819, Japan

^d Biology Department, Woods Hole Oceanographic Institution, 266 Woods Hole Rd., Woods Hole, MA, 02543, USA

ARTICLE INFO

Keywords:

Glacial fjord
Bowdoin Fjord
Zooplankton
ZooScan
NBSS

ABSTRACT

In Greenland, tidewater glaciers discharge turbid subglacial freshwater into fjords, forming plumes near the calving fronts. To evaluate the effects of this discharge on the zooplankton community in the fjords, we collected sea surface zooplankton samples in Bowdoin Fjord in north-western Greenland during the summer of 2016 and made microscopic, OPC and ZooScan analyses. Within the three quantitative methods, ZooScan has advantages that can evaluate various parameters (e.g., abundance, biomass, size and taxonomic information) simultaneously and has the ability to eliminate abiotic particles, such as silt and sediment, which are abundant in samples. Based on taxonomic biomass data, the zooplankton community is clustered into three groups, which varied spatially: inner, middle and outer fjord groups. Jellyfish dominated the outer fjord group, and barnacle cypris larvae dominated the middle fjord group. For the inner fjord group, large-sized *Calanus* spp. and chaetognaths were abundant. Since these species are characterized with oceanic taxa, they would intrude through the deep fjord water and subsequently be upwelled through entrainment of glacially modified plume water. From the NBSS analysis on zooplankton size spectra, the steep slope of NBSS in the middle fjord community suggests that the high productivity was caused by the addition of meroplanktonic cypris larvae.

1. Introduction

Recently, tidewater glaciers in Greenland have been thinning and retreating under the influence of atmospheric warming (e.g., Howat and Eddy, 2011; Murray et al., 2015). These glaciers flow directly into the ocean, forming an important ice-ocean boundary in a glacial fjord. Near the glacier front, subglacial discharge upwells and forms a sediment-rich turbid meltwater plume (Chu, 2014; Ohashi et al., 2016; Kanna et al., 2018). In front of tidewater glaciers, particularly near the plume, dense occurrences of marine mammals and sea birds are commonly observed (Hop et al., 2002; Lydersen et al., 2014; Dalpadado et al., 2016; Arimitsu et al., 2016). These aggregations of marine mammals and sea birds at meltwater plumes in glacial fjords suggest that their food, especially zooplankton, may be higher than in other regions. However, sampling and measurements are difficult near the

glacier front; thus, little information on zooplankton abundance is available in glacial fjords near the plumes.

For the evaluation of zooplankton, size and taxa are two important proxies to evaluate their quantitative and qualitative roles. Using size spectra zooplankton biomass data, calculation of normalized biomass size spectra (NBSS) provides valuable information on zooplankton productivity, energy transfer efficiency and their prey-predator linkages (Zhou, 2006; Zhou et al., 2009). While important, size measuring zooplankton by microscopic observations is time consuming. Taxonomic identification under a microscope also requires knowledge of zooplankton taxa. To overcome these problems, several instruments have been developed. An Optical Plankton Recorder (OPC) using light attenuation is an instrument that can quantify zooplankton in 4096 size categories between 0.25 and 5.0 mm using the Equivalent Spherical Diameter (ESD) in a short time (Herman, 1988, 1992). While useful, the

* Corresponding author. Graduate School of Fisheries Science, Hokkaido University, 3-1-1 Minato-cho, Hakodate, Hokkaido, 041-8611, Japan.
E-mail addresses: a-yama@fish.hokudai.ac.jp, ayamaguchi@whoi.edu (A. Yamaguchi).

¹ Present address: Nosui Co. Ltd., Mita Nitto Daibiru, 4th Floor, 3-11-36 Mita, Minato-ku, Tokyo, 108-0073, Japan.

OPC does not provide taxonomic information. An instrument that measures both size and taxonomic information at the same time, the zooplankton scanning image analysis system (ZooScan) was established (Gorsky et al., 2010). ZooScan has been used in various locations (e.g., Abrolhos Bank, Bay of Biscay, off Ubatuba, Brazil and others) (Marcolin et al., 2013, 2015; Vandromme et al., 2014). However, little information is available for inter-calibration with other instruments, which prevents the evaluation of measurement characteristics of the ZooScan.

In the present study, we studied the size and taxonomic composition of sea-surface zooplankton in Bowdoin Fjord, a glacial fjord located in north-western Greenland during July 2016. Zooplankton samples, collected by sea-surface tow at fifteen stations set from the plume to the outside along with fjord, were preserved. Using the same zooplankton samples, their size spectra were quantified by OPC and ZooScan, and taxonomic accounts were also identified with ZooScan and microscopic observations. Applying size-mass relationships, zooplankton biomass (wet mass: WM) derived by OPC and ZooScan were compared with directly measured WM. Finally, the calculation of NBSS based on OPC and ZooScan may enable us to evaluate the measurement characteristics (causes of under/over estimation) of each instrument and the regional characteristics of zooplankton in the glacial fjord.

2. Materials and methods

2.1. Field sampling

Bowdoin Glacier (77°41'N, 68°35'W) is a marine-terminating glacier located along the coast of Prudhoe Land in north-western Greenland (Sakakibara and Sugiyama, 2018). The glacier flows into Bowdoin Fjord at a rate of ~500 m year⁻¹ and discharges icebergs and meltwater through a 3-km wide calving front (Fig. 1a) (Sugiyama et al., 2015). The glacier is ~280 m thick and the fjord is ~250 m deep near the calving front. Boat-based observations were made in the daytime during 27–29 July 2016. Temperature and salinity at 2 m were measured with a CTD profiler (ASTD 102, JFE Advantech, Japan) at 44 stations, which encompassed the plume through to the outside of the fjord (data from Kanna et al., 2018). At 15 stations, a horizontal tow of a single-NORPAC net (mouth diameter 45 cm, mesh size 335 µm) at 2–3 m was made over 3 min. To register the filtered water volume, a flowmeter (Rigoshia,

Saitama, Japan) was mounted in the mouth of the net. The net sampling depth was also monitored by a depth recorder (DEFI2-D50, JFE Advantech, Japan). Zooplankton samples were preserved with borax-buffered formalin by adding 5% volume to the total zooplankton samples.

2.2. Microscopic observation and wet mass measurement

In the laboratory, microscopic observations were made of subsamples (1/4 to 1/32) made by a Motoda splitter (Motoda, 1959) according to the size of samples. Species and taxonomic identifications, sorting and counting were made under a stereomicroscope (Nikon SMZ800N). Taxa except copepods were counted with taxon (e.g. jelly-fishes, chaetognaths, appendicularians, euphausiids, polychaetes, barnacles). For copepods, classification of *Calanus* spp. and other species was made. The sorted samples were placed on pre-weighed mesh (100 µm), seawater was removed with aid of tissue, then the wet mass (WM) was measured with a microbalance (Mettler Toledo AE100) with the precision of 0.1 mg. All abundance and biomass data are shown as per cubic metre (ind. m⁻³ or mg WM m⁻³).

2.3. OPC measurement

OPC measurements were made with a bench-top OPC (Model OPC-1L: Focal Technologies Corp.) using 1/2–1/128 subsamples (varied according to the size of the samples) of the total formalin-preserved samples. OPC measurements were made at a low flow rate (ca. 10 L min⁻¹) and low particle density (< 10 counts s⁻¹) without staining (Yokoi et al., 2008).

The abundance per cubic metre (N : ind. m⁻³) for each of the 4096 ESD size categories was calculated using the following equation:

$$N = \frac{n}{s \times F}$$

where n is the number of particles (= zooplankton ind.), s is the split factor of each sample, and F is the filtered volume of the net (m³). The biovolume of the zooplankton community in 4096 size categories was calculated from the ESD data, and the biovolume (mm³ m⁻³) was calculated by multiplying N and the volume (mm³ ind.⁻¹) derived from

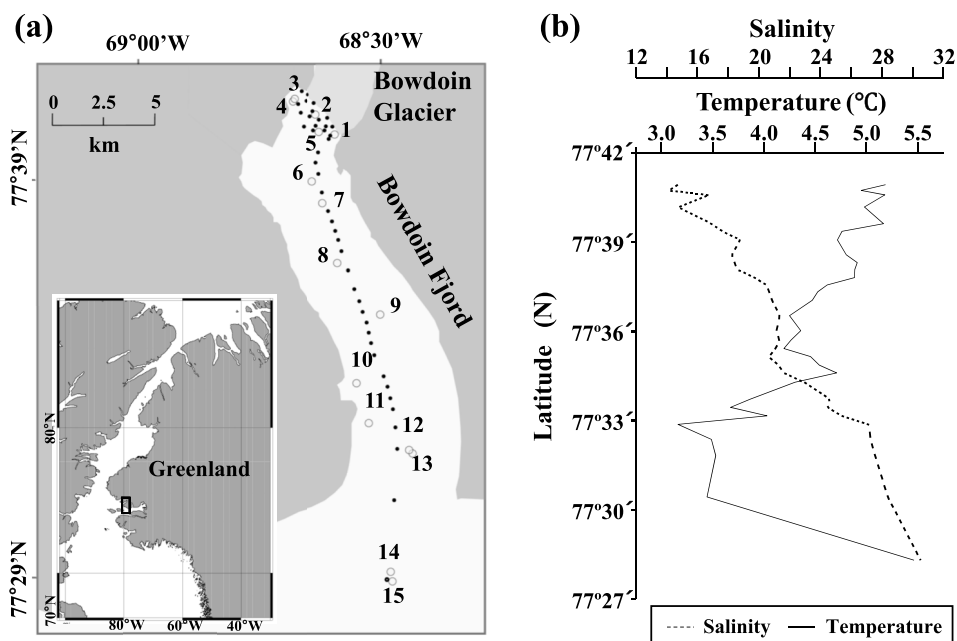


Fig. 1. Sampling location (a) and latitudinal changes in hydrography (temperature and salinity) (b) in Bowdoin Fjord during 27–29 July 2016. Open symbols: plankton sampling, dotted symbols: CTD measurement.

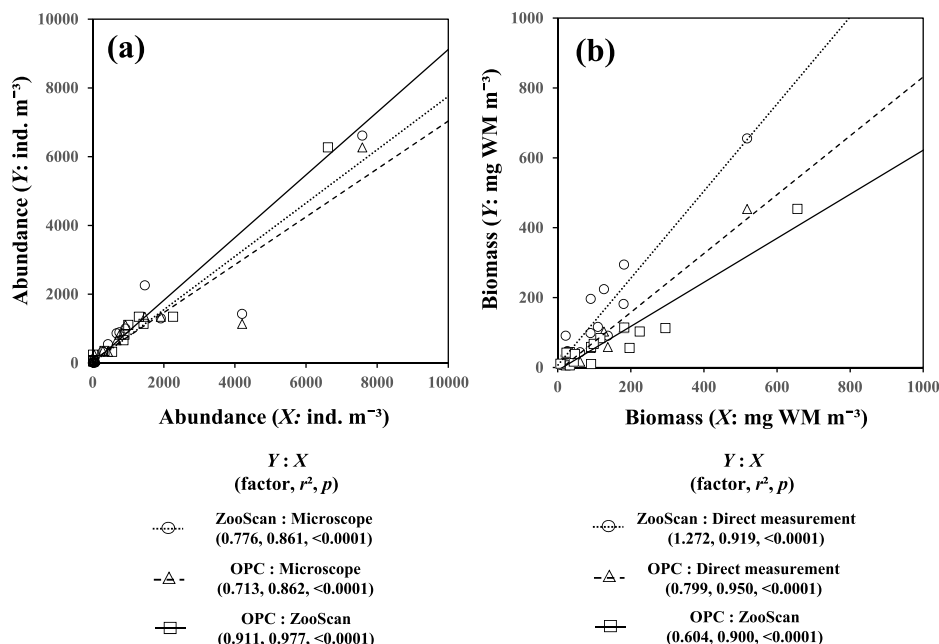


Fig. 2. Linear regressions of abundance (a) and biomass (b) of the total zooplankton community between different quantitative methods: microscopic count, direct wet mass (WM) measurement, OPC and ZooScan measurements. Each regression indicates the linear fit between one method (Y-axis) versus another method (X-axis). Factor means Y:X.

ESD. Zooplankton wet mass (WM) for 4096 size categories was calculated from the ESD data by assuming the relative density of zooplankton to be equal to that of seawater (1 mg mm^{-3}). Analyses of the meso-zooplankton biomass were performed with the separation of five size classes (0.335–1 mm, 1–2 mm, 2–3 mm, 3–4 mm, 4–5 mm ESD).

2.4. ZooScan measurement

Zooplankton images were scanned with a water-proof ZooScan (ZooScan MIII, Hydroptic Inc., France) using 1/4–1/128 subsamples (varied according to the size of the samples) of the total formalin-preserved samples. The overall process and analysis followed Gorsky et al. (2010). Before each measurement, background measurements were made by filling with deionized water. ZooScan measurements were made under the condition that all zooplankton sank to the bottom of a scanning cell of $15 \text{ cm} \times 24 \text{ cm}$ in area. Zooplankton overlapping was avoided by using soft tweezers manually.

The obtained zooplankton images were separated from individual objects by the ZooProcess software. Zooplankton images were digitalized at 2400 dpi resolution. From this resolution, one pixel corresponded to $10.58 \mu\text{m}$. For identification, all obtained images were uploaded to the website EcoTaxa (<http://ecotaxa.obs-vlfr.fr/prj/>). Images, identified as “detritus”, “fibre”, “artifact” and “other”, were removed for further analyses. ZooScan provides estimates of body length (major axis of the best fitting ellipse) and width (minor axis) (Gorsky et al., 2010). From these major and minor axes, the biovolume was calculated: $\text{biovolume} = 4/3 \times \pi \times (\text{major axis}/2) \times (\text{minor axis}/2)^2$. From these biovolume data, the equivalent spherical diameter (ESD, μm) was computed for each zooplankton object. Zooplankton wet mass (WM) was calculated from the ESD data by assuming the relative density of zooplankton to be equal to that of seawater (1 mg mm^{-3}).

2.5. Data analysis

To evaluate regional changes in the zooplankton community, a cluster analysis based on biomass was performed. Zooplankton biomass data (ZB: mg WM m^{-3}) of each taxon (jellyfishes, chaetognaths, appendicularians, euphausiids, polychaetes, barnacles, *Calanus* spp. and other copepods) were normalized as $\log_{10}(\text{ZB} + 1)$. Next, similarities between zooplankton samples were calculated using the Bray-Curtis similarity index. To group the samples, similarity indices were coupled

with hierarchical agglomerative clustering using a complete linkage method (Unweighted Pair Group Method using Arithmetic mean: UPGMA; Field et al., 1982). These analyses were made with PRIMER v7 (PRIMER-E Ltd.).

From OPC and ZooScan data, zooplankton biovolume ($\text{mm}^3 \text{ m}^{-3}$) class interval. 0.335 and 5.0 mm ESD was summed at each 0.1-mm ESD size class interval. To calculate the X-axis of the NBSS (X: \log_{10} zooplankton biovolume [$\text{mm}^3 \text{ ind.}^{-1}$]), the biovolume was divided by the abundance of each size class (ind. m^{-3}) and converted to a common logarithm. To calculate the Y-axis of the NBSS (Y: \log_{10} zooplankton biovolume [$\text{mm}^3 \text{ m}^{-3}$]/ Δ biovolume [mm^3]), the biovolume was divided by the interval of biovolume (Δ biovolume [mm^3]) and converted to a common logarithm. Based on these data, the NBSS linear model was calculated as follows:

$$Y = aX + b$$

Where a and b are the slope and intercept of the NBSS, respectively.

To make comparisons of NBSS between OPC and ZooScan, a U test was made. To evaluate whether the NBSS slope varied with the NBSS intercept or measured instruments, an analysis of covariance (ANCOVA) with the NBSS intercept and measured instruments (OPC or ZooScan) as independent variables was conducted. U test analyses and an ANCOVA were performed using StatView v5 (SAS Institute Inc., Cary, NC, USA).

3. Results

3.1. Hydrography

Temperature at the 2-m depth ranged between 3.16 and 5.21 °C, and decreased from the glacier to outer fjord, while it showed abrupt high temperatures at the farthest offshore station (Fig. 1b). Salinity was in the range of 13.62 – 30.52 and increased from the glacier plume to the outer fjord.

3.2. Calibration

Comparisons of abundance (ind. m^{-3}) and WM (mg WM m^{-3}) between OPC or ZooScan-derived data and direct measurements were made (Fig. 2). Based on whole samples ($n = 15$), all measurements were highly correlated with each other ($r^2 = 0.86$ – 0.95 , $p < 0.0001$).

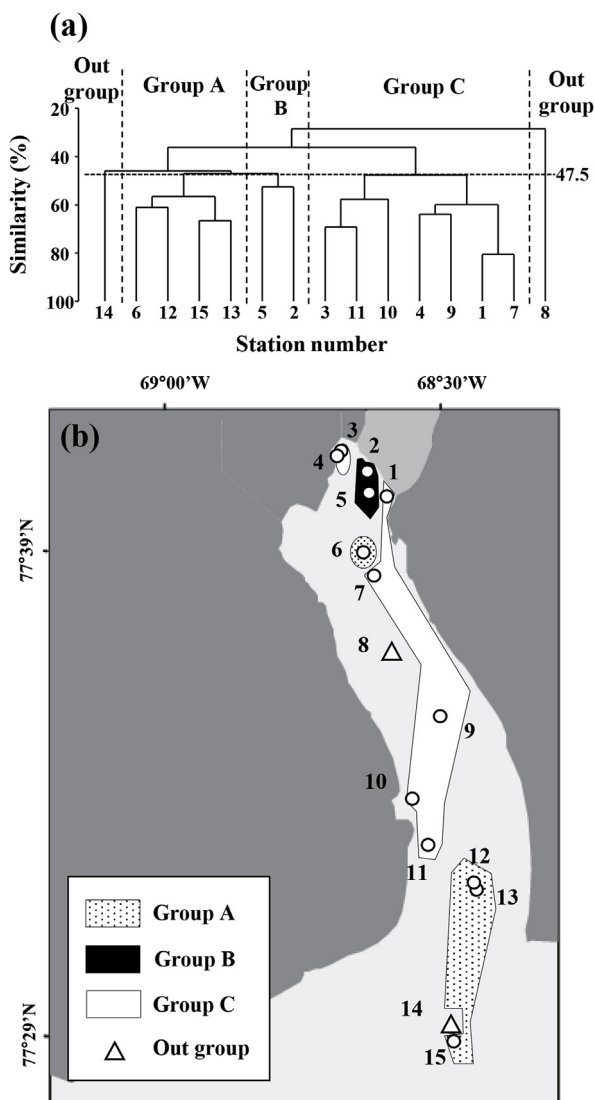


Fig. 3. Results of a cluster analysis based on zooplankton biomass derived from wet mass measurement (a). Three groups (A–C) and two out groups (Out) were identified at 47.5% similarity. The horizontal distribution of each group identified from cluster analysis on zooplankton biomass in the Bowdoin Fjord during 27–29 July 2016 (b).

For abundance, both OPC and ZooScan underestimated more than microscopic observations (by a factor of 0.71–0.78), while OPC:ZooScan had similar values (0.91) (Fig. 2a). For biomass, while coefficients of determination were high ($r^2 = 0.90$ – 0.95), differences due to measurement methods were greater than those for abundance. Thus, within the same samples, ZooScan quantified the largest value, followed by direct measurements, and OPC yielded the least value (Fig. 2b).

3.3. Cluster analysis

Based on directly measured zooplankton biomass, the zooplankton community was separated into three groups (A, B and C) at 47.5% similarity (Fig. 3a). The horizontal distribution of each group varied clearly (Fig. 3b). Thus, group A was mainly observed in the outer fjord, while group B was concentrated at the centre of the plume in front of the glacier. The other largest group C mainly occupied the middle of the fjord. For each group, the dominant zooplankton taxa varied: jellyfishes dominated in group A, chaetognaths and copepods dominated in group B, and barnacle larvae (cypris) dominated in group C (Fig. 4).

3.4. Inter-method comparison in taxa (ZooScan vs microscope)

Within the three quantitative methods (OPC, ZooScan and microscope), taxonomic information was obtained from the ZooScan and by the microscope. Subsequently, combining directly measured WM with taxa, the taxonomic composition of zooplankton abundance and biomass were compared between those from ZooScan and direct quantification. The abundance showed little differences between direct measurement and ZooScan (Fig. 4). On the other hand, biomass showed overestimation/underestimation, which varied with taxa and station (Fig. 4).

Abundance showed significant correlations between ZooScan and microscopic observations for all species/taxa, while biomass showed significant correlations for only four taxa, which accounted for half of the eight taxa (Fig. 5). In detail, for abundance, appendicularians, euphausiids and copepods (*Calanus* spp. and others) had nearly linear ($Y:X = 0.97$ – 1.03) correlations between the ZooScan and microscopic observations, while jellyfishes, chaetognaths, polychaetes and barnacle larvae were underestimated by ZooScan, with factors of 0.29–0.78 (Fig. 5). For biomass, while four taxa showed significant correlations between ZooScan and direct measurements, their factors in ZooScan were overestimations (1.26–2.94) for polychaete and barnacle larvae and underestimations (0.22–0.33) for appendicularians and other copepods.

3.5. Inter-method comparison in size (ZooScan vs. OPC)

Zooplankton size properties in abundance and biomass were quantified by two methods: OPC and ZooScan. For abundance, both methods showed the predominance of the smallest size class (0.335–1 mm ESD) throughout the stations and had little differences with quantitative methods (Fig. 6). On the other hand, for biomass, differences between methods were detected. Thus, zooplankton group A was dominated by the small size class in OPC, while it was dominated by the large size class in ZooScan. For zooplankton group C, the opposite pattern was seen: i.e., dominance of the large size class in OPC, while predominance of the small size class in ZooScan was observed (Fig. 6).

Comparison within size classes showed that the smallest size class (0.335–1 mm ESD) was highly correlated between ZooScan and OPC both in abundance and biomass (Fig. 7). For the other size classes, significant correlations were observed for the 2–3 mm size class in abundance and the 1–2 and 2–3 mm size classes in biomass. Common patterns for these size classes were underestimations of ZooScan compared to OPC, with factors of 0.21–0.28 (Fig. 7).

3.6. Inter-method comparison in NBSS (ZooScan vs OPC)

The results of the NBSS analysis based on OPC and ZooScan are shown in Table 1. Slopes of NBSS based on OPC were -1.705 to -0.737 (mean \pm sd: -1.111 ± 0.301) and those by ZooScan were -1.516 to -0.229 (-0.778 ± 0.394). Slopes of NBSS were more moderate for ZooScan than those from OPC (U test, $p < 0.05$) (Fig. 8). Intercepts of NBSS based on OPC were -1.306 to -0.245 (-0.736 ± 0.352), and those by ZooScan were -1.326 to -0.889 (-0.726 ± 0.537). No significant differences were detected for intercepts of NBSS between OPC and ZooScan (U test, $p = 0.958$). From NBSS plots, it was notable that zooplankton biovolumes at smaller size classes were lower for ZooScan than for OPC (Fig. 8). This was due to the elimination of abiotic particles (e.g., silt or sand) from ZooScan data based on the imaging analysis. For NBSS slopes, an ANCOVA analysis, applying NBSS intercepts and differences in instruments (OPC or ZooScan) as the independent variables, detected significant differences only for the differences in the instruments (Table 2).

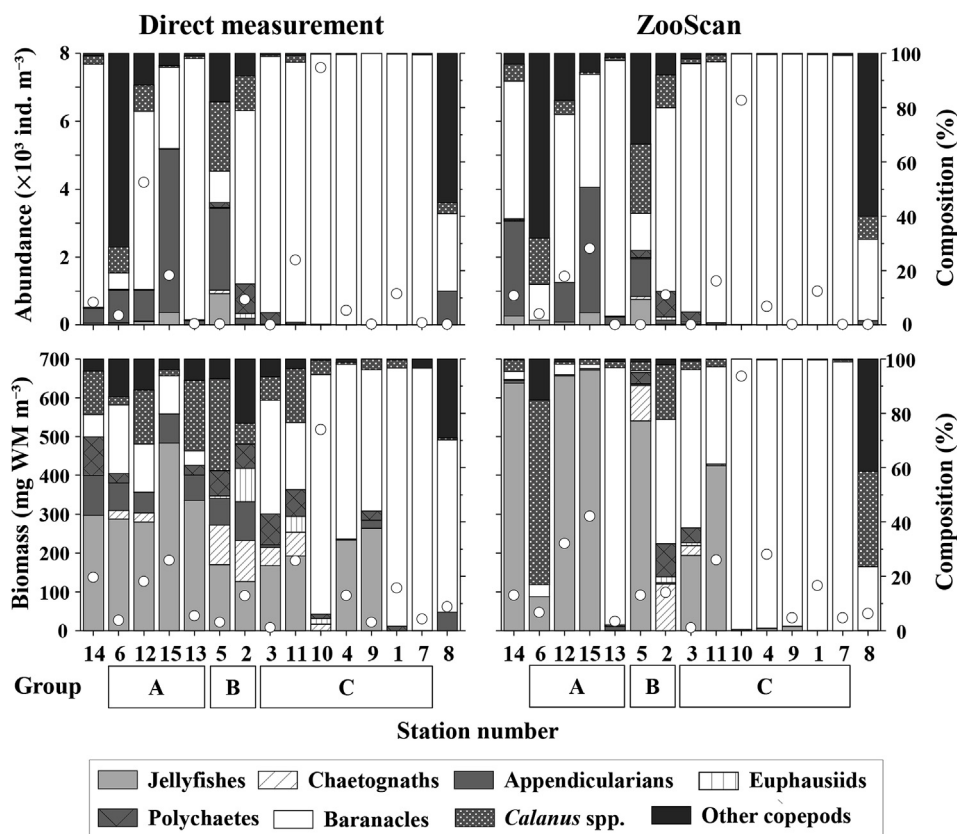


Fig. 4. Comparison of abundance, biomass and taxonomic composition, which was quantified by microscopic count and direct measurements (left), and those by ZooScan measurements (right). Labels (Group A-C) below station numbers indicate clustered groups (cf. Fig. 3a).

4. Discussion

Through zooplankton sample analyses based on multiple methods (i.e., microscope, WM, OPC and ZooScan measurements), various characteristics in the zooplankton community in the glacial fjord were evaluated. In the following section, we discuss three methodological notes in terms of taxonomic (ZooScan vs microscope), size and NBSS (ZooScan vs OPC) first. Then, we discuss the factors governing zooplankton community in the glacial fjord.

4.1. Taxonomic comparison

While important, taxonomic information of zooplankton was not quantified in optical instruments such as OPC and LOPC (Herman, 1988; Nogueira et al., 2004). ZooScan obtains images of zooplankton and quantifies both size and taxonomic data from images (e.g., Vandromme et al., 2012). In this section, we compare taxonomic data from ZooScan with microscopic counts (abundance) and direct WM measurements (biomass).

Zooplankton abundance based on ZooScan have pointed out the possibility of underestimation of minor taxa/species due to the deviation or split of the samples (Colas et al., 2018). As a quantification method for minor and large-sized species/taxa, gently sieving through a 0.5-mm mesh and ZooScan measurements for each fraction have been proposed (Grosjean et al., 2004). However, it requires twice the time and is difficult to achieve for many samples (Colas et al., 2018). Underestimation of abundance due to the use of subsamples is reported to be common for rare species/taxa (Gorsky et al., 2010). This is considered to be the cause of the underestimation of abundance for two less abundant taxa: jellyfishes and chaetognaths in this study (Fig. 5), while underestimations for numerical dominant two taxa, polychaetes and barnacle larvae, would be caused by the double-splitting effects (note

that the splitting was available for both microscopic counts and ZooScan measurements) or heterogeneous distribution of these taxa in the samples.

For zooplankton abundance, a good correlation has been reported for automated and manual analyses based on same images created by ZooScan (Gorsky et al., 2010), while for zooplankton biomass, comparison between estimated values from ZooScan measurements and directly measured mass have not been reported to date. For biomass estimation using ZooScan, underestimation tends to occur for large-body sized organisms and taxa through the use of subsamples, since they are rare (e.g., termed “subsample effect”, cf. Colas et al., 2018). Fluctuations of ZooScan-derived biomass of chaetognaths and euphausiids in this study would be caused by this subsample effect (Fig. 5). Interestingly, clear underestimation by ZooScan for appendicularian biomass occurred in this study (Fig. 5). This may be due to the shape of appendicularian tails, which are often curved, affecting the automated measurements (Gorsky et al., 2010). The transparency of appendicularians may also affect the underestimation of their biomass (Herman, 1992). Concerning jellyfishes, the destruction of fragile organisms and species-specific differences in colour (=differences in transparency) may affect size measurements (Thompson et al., 2013). While a significant correlation pattern was not detected in this study, zero or overestimation were the cases for jellyfishes (Fig. 5). This may be due to the underestimation by transparent body or overestimation of size due to the extension of jellyfish bodies on the measurement frame of ZooScan. For polychaetes and barnacles, the two overestimated taxa for ZooScan biomass, since most of them were small sized meroplanktonic larvae, it is difficult to accurately measure the wet mass using this method in this study. Thus, underestimation of directly measured wet mass would be the case for these two taxa.

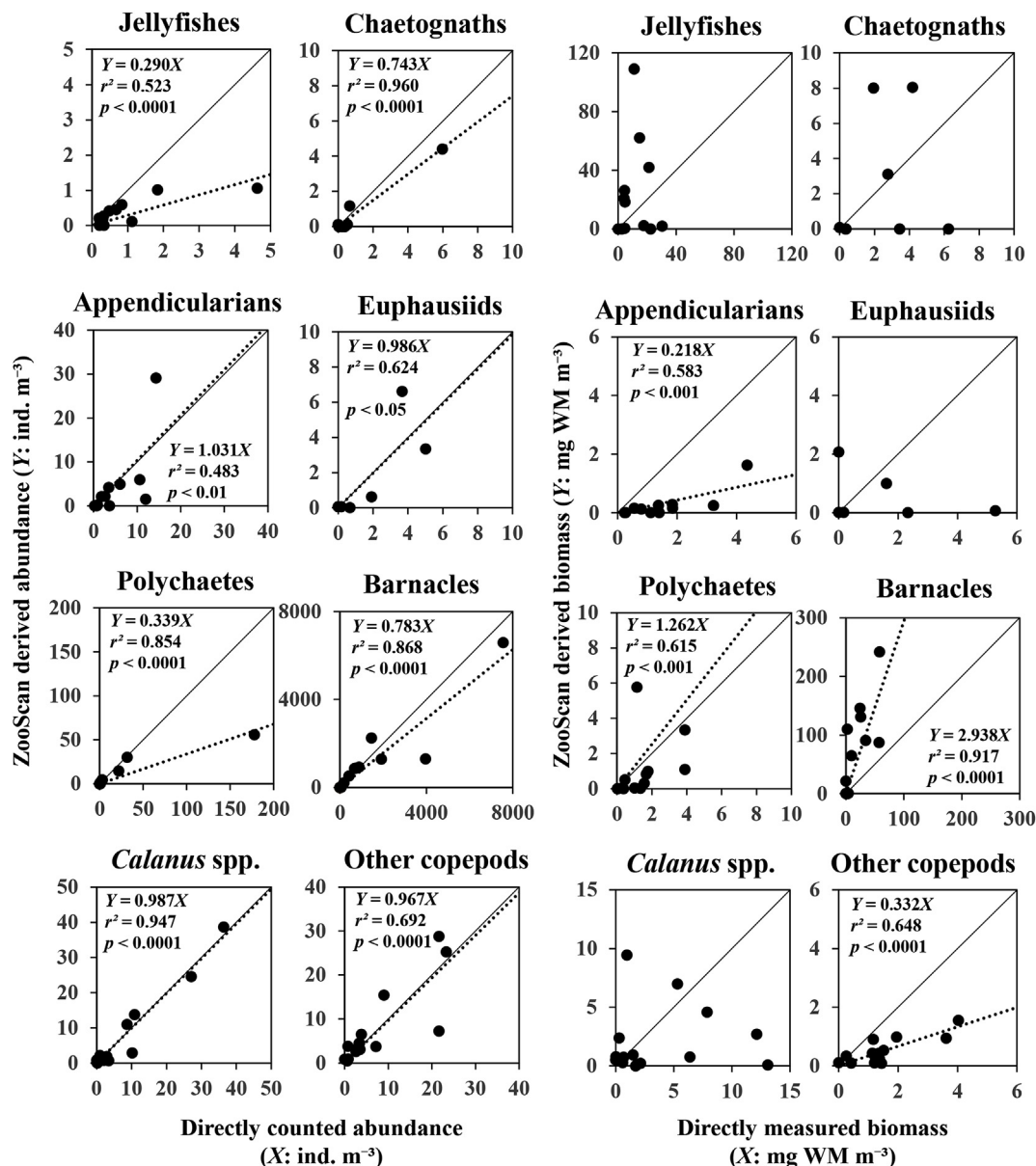


Fig. 5. Relationships between ZooScan (Y-axis) and direct quantification (X-axis) on the abundance and biomass of each zooplankton species/taxon. Solid and dashed lines indicate 1:1 and significant relationships between the values, respectively.

4.2. Size comparison

In this study, the size property of zooplankton was measured by OPC and ZooScan. OPC measures the size of plankton by detecting the shade of planktonic particles created by a light beam and quantified size with 4096 size units (Herman, 1992). Since OPC detects particle as shadows during flow through a channel, there are some potential sources of underestimation and overestimation on counting or sizing. As the cause of underestimation, underestimation in number by particle coincidence and underestimation in size caused by zooplankton direction to the light beam or body transparency are argued (Herman, 1992; Sprules et al., 1998; Zhang et al., 2000). Conversely, as the cause of overestimation, overestimation in number by counting on non-zooplankton particles, such as detritus and fragmentation of zooplankton body and overestimation in size by particle coincidence, are reported (Sprules et al., 1998; Zhang et al., 2000). For ZooScan, since ZooScan quantifies the biovolume of zooplankton by assuming a perfect spheroid shape, their estimated biomass is reported to be constantly higher than those measured by OPC (Schultes and Lopes, 2009). With such shortcomings,

zooplankton biomass estimation by ZooScan is preferred to those of OPC because of the elimination of the aforementioned various under- and overestimations, which are inevitable for OPC measurements (Schultes and Lopes, 2009).

In the present study, correlations between OPC and ZooScan were detected for both abundance and biomass of the relatively small size classes (0.335–3 mm) (Fig. 7). Within them, highly significant correlations ($r^2 = 0.99$, $p < 0.0001$) were observed for the smallest size fraction (0.335–1 mm). In detail, the abundance showed nearly an equal factor between them (1.04), while the biomass of ZooScan was 1.44 times higher than that of OPC. This discrepancy would be caused by the differences in the biovolume measurement method in ZooScan (by assuming a perfect spheroid shape) mentioned above (Schultes and Lopes, 2009), while in the 1–3 mm size classes, a considerable underestimation by ZooScan (with a factor of 0.21–0.28 of OPC) occurred for both abundance and biomass (Fig. 7). For OPC, overestimations of abundance and biomass frequently occurred by including detritus count (overestimation in abundance) and size measurements on overlapping particles through a light beam (overestimation in biomass) (Sprules

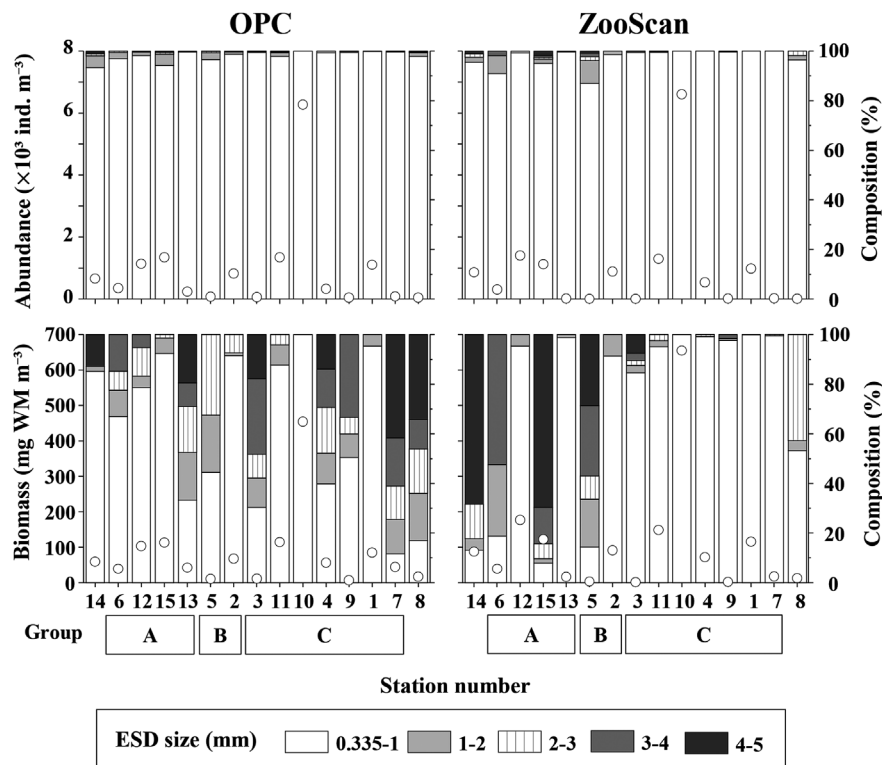


Fig. 6. Comparison of abundance, biomass and size composition, which were quantified by OPC (left) and ZooScan (right). Sizes were arranged with five ESD size classes between 0.335 and 5 mm (0.335–1, 1–2, 2–3, 3–4, 4–5 mm). Labels (Group A–C) below station numbers indicate clustered groups (cf. Fig. 3a).

et al., 1998; Zhang et al., 2000). On the other hand, ZooScan can avoid the overlapping of particles by manual manipulation before measurement and can remove detrital material data through image analysis. In fact, we confirmed that detrital materials were composed $88.2 \pm 12.7\%$ of total particles (including both plankton and detritus) in 1–3 mm size classes by ZooScan image analysis. Thus, removing data on detrital materials may cause a greater underestimation of ZooScan than the data of OPC, which includes whole particles (both plankton and detritus). These facts suggest that ZooScan can provide more accurate data on plankton. Because of the lack of correlation detected for large size classes (3–5 mm), since these large size classes contain few individuals, variations due to sample split may induce the great variability in the individuals who belong to these size classes.

4.3. NBSS

NBSS is a calculated linear expression based on zooplankton size and is treated as an index of the status of marine ecosystems (Herman and Harvey, 2006; Marcolin et al., 2015). The slope of NBSS represents zooplankton productivity, energy transfer efficiency and their prey-predator linkages (Zhou, 2006; Zhou et al., 2009). The intercept of NBSS is an index of standing stocks (Sprules and Munawar, 1986). The slope of NBSS at approximately -1 indicates a theoretical steady state (Sprules and Munawar, 1986). In general, slopes steeper than -1 indicate bottom-up control (Moore and Suthers, 2006), or high productivity with low transfer efficiency (Sprules and Munawar, 1986; Zhou, 2006). Slopes flatter than -1 indicate top-down control (Moore and Suthers, 2006), or low productivity with high transfer efficiency (Sprules and Munawar, 1986; Zhou, 2006).

Since the ZooScan analysis is based on images, abiotic materials such as silt and sand are able to be eliminated before analysis (Gorsky et al., 2010). On the other hand, OPC could not separate plankton and abiotic particles. From the NBSS slope comparison between ZooScan and *in situ* LOPC in the Bay of Biscay, Vandromme et al. (2014) reported that the NBSS slope by LOPC (mean \pm 1 sd: -0.97 ± 0.24) is steeper

than those by ZooScan (-0.86 ± 0.40), while in a similar comparison in the Abrolhos Bank, Marcolin et al. (2013) reported the opposite pattern: i.e., the NBSS slope of LOPC is slightly flatter than those of ZooScan. These differences would be caused by the differences in the dominant zooplankton taxa, community structure and treated size ranges. In the present study, we applied the same size ranges for the NBSS calculation of both ZooScan and OPC and eliminated abiotic particle data for the NBSS calculation of ZooScan. This approach provides high biomass values for OPC, especially at small sizes, and steeper slopes for OPC (-1.11 ± 0.30) than those of ZooScan (-0.78 ± 0.39) (Fig. 8).

For the intercept of NBSS, because of the overestimation in fragmentation of jellyfishes during course of quantification, *in situ* LOPC tends to overestimate more than those of ZooScan (Vandromme et al., 2014). In this study, the intercept of NBSS showed no significant differences between those from OPC (mean \pm 1 sd: -0.74 ± 0.35) and ZooScan (-0.73 ± 0.54) (*U* test, $p = 0.958$). This finding may be observed because the abiotic particles eliminated from ZooScan analysis were mostly at smaller sizes, and their elimination had little effect on the NBSS intercept. Commonly, the NBSS intercept is correlated with the NBSS slope (cf. Matsuno et al., 2012). However, in this study, the NBSS slope has no correlation with the intercept, but has a correlation with the instrument (e.g., OPC or ZooScan) (Table 2). These facts suggest that the effect of elimination of abiotic particles in the ZooScan analysis may have a greater effect on the results of the NBSS slope. Thus, to make an accurate evaluation of the NBSS slope, NBSS calculations based on ZooScan, including elimination of abiotic particles, are recommended.

4.4. Zooplankton community in the fjord

For zooplankton community, it should be noted that our data is only a surface sampling. Data interpretation by the differences of the sampling method from the previous studies should be considered. In glacial fjords, the zooplankton community is known to be strongly affected by

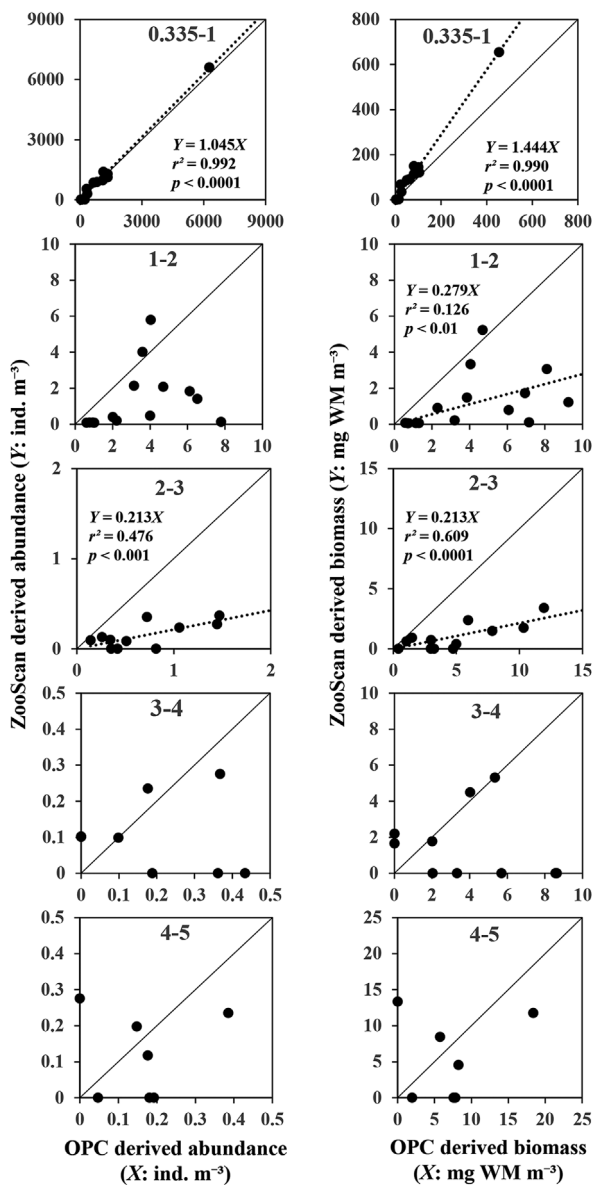


Fig. 7. Relationships between abundance (left) and biomass (right) derived from ZooScan (Y-axis) and OPC (X-axis) of each zooplankton ESD size class (0.335–1, 1–2, 2–3, 3–4 and 4–5 mm). Solid and dashed lines indicate 1:1 and significant relationship between the values, respectively.

the advection of outer oceanic water (Aksnes et al., 1989). For instance, the composition of the oceanic copepod *Calanus* spp. is increased through the outer fjord and accounted for 90% of their biomass (Arendt et al., 2010). In the present study, zooplankton biomass in the outer fjord (group A) was dominated by jellyfishes, and the composition of *Calanus* spp. was low (0.56–9.59%) (Figs. 3 and 4). For this reason, the sampling methods of this study (horizontal net tow at sea surface [2–3 m]) may also be considered. Concerning jellyfishes, the dominance of the jellyfishes for the water masses outside the fjord are reported (Palma et al., 2014). Bearing this in mind, the dominance of jellyfishes outside the fjord yield their dominance for zooplankton community group A.

For the zooplankton community in the middle of the fjord in Greenland, various copepods were dominant: *Metridia longa*, *Pseudocalanus* spp., *Microsetella* spp. and *Oncaea* spp. have been reported (Arendt et al., 2010; Swalethorp et al., 2015). However, in the present study, the zooplankton biomass of group C, observed in the middle of the fjord, was dominated by barnacle cypris larvae (Figs. 3

Table 1

List of NBSS slope and intercept derived from OPC and ZooScan at each station in the Bowdoin Fjord during 27–29 July in 2016.

Station	NBSS derived from OPC			NBSS derived from ZooScan		
	Slope	Intercept	r^2	Slope	Intercept	r^2
1	-1.096	-0.762	0.608	-1.130	-0.597	0.520
2	-1.110	-0.415	0.877	-0.995	-0.697	0.686
3	-1.136	-0.368	0.806	-1.077	-0.451	0.739
4	-1.551	-0.578	0.882	-1.390	-0.407	0.650
5	-0.942	-0.656	0.931	-0.516	-1.005	0.732
6	-1.012	-1.179	0.915	-0.602	-1.326	0.720
7	-1.222	-0.639	0.751	-0.744	-0.685	0.137
8	-0.828	-1.258	0.832	-0.358	-1.168	0.427
9	-1.242	-0.262	0.835	-0.839	-0.443	0.385
10	-1.705	-0.245	0.607	-0.229	0.889	0.008
11	-0.868	-0.581	0.809	-0.997	-0.774	0.515
12	-0.905	-1.306	0.850	-0.406	-1.154	0.361
13	-1.562	-0.784	0.816	-1.516	-0.836	0.561
14	-0.747	-0.884	0.908	-0.446	-1.088	0.565
15	-0.737	-1.121	0.866	-0.433	-1.164	0.715

and 4). Concerning cypris larvae in the fjord environment, Swalethorp et al. (2015) reported that cypris larvae were abundant in the outer fjords in Greenland. These discrepancies may be related to differences in sampling period (June or July), latitude (77.5°N vs 64–65°N) and currents in each fjord. In the present study, the slope of the NBSS of group C (-0.915 ± 0.368) was steeper than those of the other groups (-0.745 ± 0.434) (Fig. 8 and Table 1). It suggests that high productivity occurred in the middle of the fjord. The steeper NBSS slope of group C would be caused by the dominance of small-sized cypris larvae. Since meroplanktonic larval phase of barnacles is limited for 2–3 weeks (Herz, 1933), these steeper NBSS slopes of group C in the middle of the fjord would be moderate, and the productivity would decrease after one month of this study.

For the inner fjords near glaciers in Greenland, the dominance of the copepods *M. longa* and *Pseudocalanus* spp. has been reported (Swalethorp et al., 2015). This may due to high biomass of their prey: i.e., protozooplankton, rotifer and copepod nauplii are available there, and it implies favourable food conditions for copepods (Calbet et al., 2011; Riisgaard et al., 2014; Swalethorp et al., 2015). Since there is a high gradient of suspended particulate matter in inner fjords, species-specific differences in tolerance for high sediment loads may explain their distribution (Arendt et al., 2011). For the glacial fjord, subglacial discharge upwells and forms a sediment rich turbid meltwater plume (Chu, 2014). In the plume, high concentrations of suspended materials may affect feeding, egestion and reproduction of copepods. The ability to tolerate sediment is likely high for *M. longa* and low for *Calanus* spp., which determine their horizontal distribution; i.e., *M. longa* and *Calanus* spp. occurred in the inner fjords and outer ocean, respectively (Arendt et al., 2011).

In glacial fjords, the input of glacial meltwater provides nutrients and induces high primary production in the inner parts of the fjord (Arendt et al., 2010). In our study region of Bowdoin Fjord, tidewater glaciers discharge turbid subglacial freshwater into fjords, forming a plume and providing macronutrient by upwelling near the calving front (Kanna et al., 2018). Through enhanced primary production, high productivity of zooplankton is expected in front of the glacier. However, the slope of NBSS for zooplankton group B, which was observed near the glacier, did not vary with the other groups ($p = 0.769$, one-way ANOVA). This indicates moderate zooplankton productivity there. Concerning taxonomic composition, the zooplankton community of group B contained a high composition of *Calanus* spp. and chaetognaths, instead of the reported species/taxa (e.g., *M. longa* and *Pseudocalanus* spp.). Since both *Calanus* spp. and chaetognaths are characterized with oceanic species (Arendt et al., 2010), the occurrence of them near the calving front in this study suggests that there was inflow from

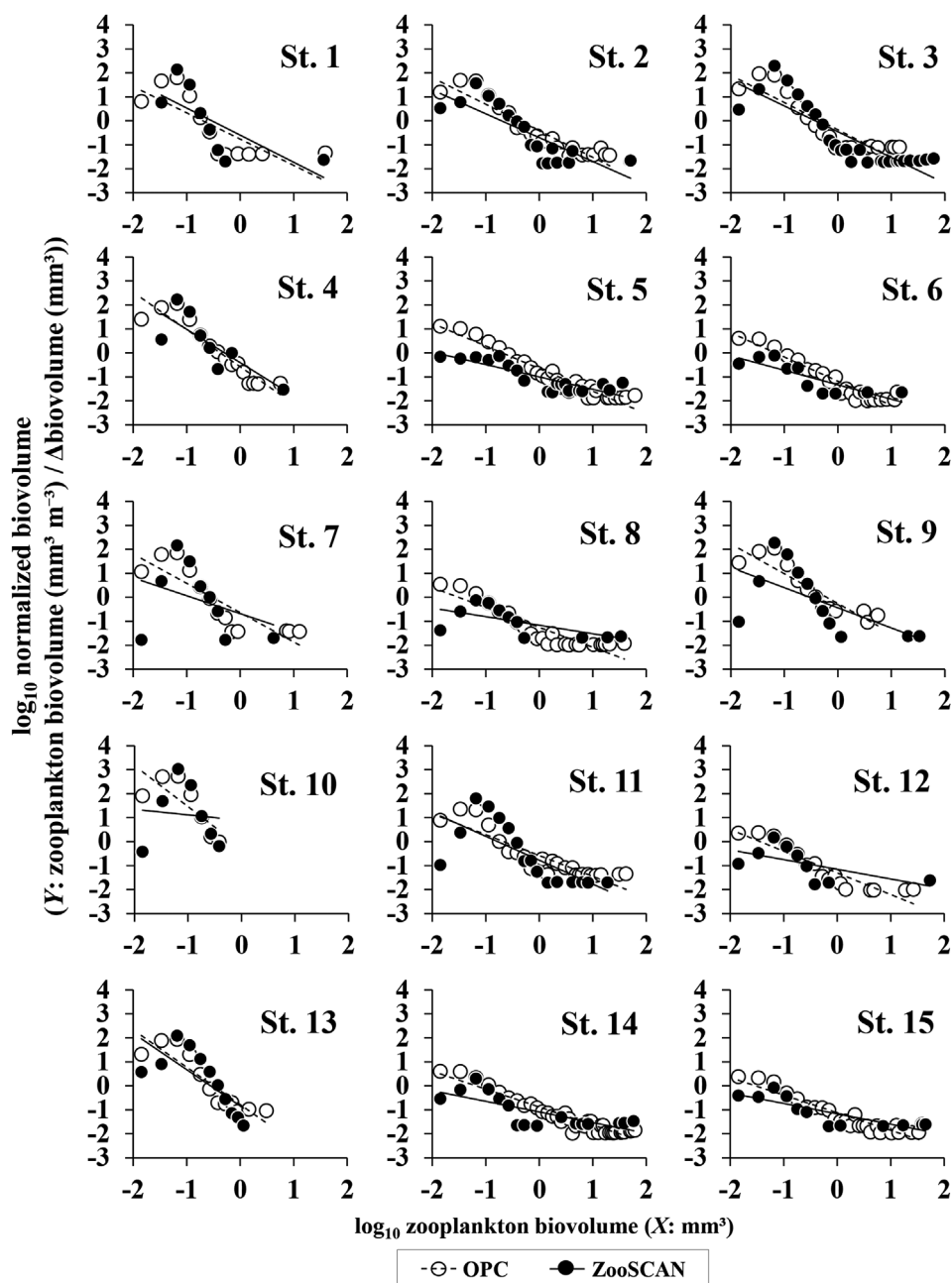


Fig. 8. NBSS for zooplankton at each station in the Bowdoin Fjord during 27–29 July 2016. Open and solid symbols are the plots derived from OPC and ZooScan, respectively. Dashed and solid lines are the fitted plots of NBSS for OPC and ZooScan, respectively.

Table 2
Results of ANCOVA for the slope of NBSS, with the intercept of NBSS and differences in instrument (i.e., OPC or ZooScan) applied as independent variables.

Parameter	d.f.	SS	F-value	p-value
Intercept	1	0.304	2.423	0.1316
Instrument	1	0.304	6.538	0.0167
Instrument × Intercept	1	0.311	2.477	0.1276

oceanic water through the bottom of the fjord and upwelling by plume in front of the glacier. In fact, upwelling of deep water in front of glacier has been reported for Bowdoin Fjord (Kanna et al., 2018). Since the sediment tolerance of *Calanus* spp. is low (Arendt et al., 2011), it may be hard for them to live in the inner fjord. Due to the large body size

and high nutrition, the carcasses of *Calanus* spp. and chaetognaths would be a good food sources for fishes (Arctic cod) and surface feeding sea birds (Black-legged Kittiwake *Rissa tridactyla*, Glaucous Gull *Larus hyperboreus* and Northern Fulmar *Fulmarus glacialis*), which form massive aggregations at the calving front of the Bowdoin Fjord (Nishizawa et al., submitted).

5. Conclusions

Based on zooplankton samples collected at the surface of Bowdoin Fjord in north-western Greenland, the zooplankton community structure was evaluated using three methods: a microscope, OPC and ZooScan. Among these methods, the analysis by ZooScan was able to filter out abiotic particles. Because of this advantage, it was shown that ZooScan provides more accurate abundance, biomass, size composition and NBSS data than the previously applied microscopic analysis, direct

wet mass measurements and OPC measurements. Through analyses, the zooplankton community was clustered into three groups that characterized differences in dominant taxa. The horizontal distribution of the three groups clearly separated each other. The outer groups were dominated by jellyfishes, the middle fjord group was dominated by cypris larvae of barnacles, and the inner groups was characterized by large-sized *Calanus* spp. and chaetognaths. The large-sized zooplankton of the inner group suggests that they were transported from the outer fjord through layers of bottom water, then upwelled by the plume near the calving glacier. Since the large zooplankton contain more nutrition than the zooplankton of the other two groups, the inner fjord near the calving front would be a good feeding ground for fish and sea-birds.

Acknowledgements

We thank Toku Oshima and Drs. Yasushi Fukamachi, Yoshihiko Ohashi, Daiki Sakakibara and Izumi Asaji, who assisted with our field observations. This study was financially supported by the Arctic Challenge for Sustainability (ARCS) project led by Drs. Kumiko Azuma and Toru Hirawake. Part of this study was supported by a Grant-in-Aid for Scientific Research 18K14506 (Early Career Scientists), 17H01483 (A), 16H02947 (B) and 15KK0268 (Joint International Research) from the Japan Society for the Promotion of Science (JSPS).

Appendix A. Supplementary data

Supplementary data to this article can be found online at <https://doi.org/10.1016/j.polar.2019.01.001>.

References

- Aksnes, D.L., Aure, J., Kaartvedt, S., Magnesen, T., Richard, J., 1989. Significance of advection for the carrying capacities of fjord populations. *Mar. Ecol. Prog. Ser.* 50, 263–274.
- Arendt, K.E., Nielsen, T.G., Rysgaard, S., Tønnesson, K., 2010. Differences in plankton community structure along the Godthåbsfjord, from the Greenland Ice Sheet to offshore waters. *Mar. Ecol. Prog. Ser.* 401, 49–62.
- Arendt, K.E., Dutz, J., Jónasdóttir, S.H., Jung-Madsen, S., Mortensen, J., Møller, E.F., Nielsen, T.G., 2011. Effects of suspended sediments on copepods feeding in a glacial influenced sub-Arctic fjord. *J. Plankton Res.* 33, 1526–1537.
- Arimitsu, M.L., Piatt, J.F., Mueter, F., 2016. Influence of glacier runoff on ecosystem structure in Gulf of Alaska fjords. *Mar. Ecol. Prog. Ser.* 560, 19–40.
- Calbet, A., Riisgaard, K., Saiz, E., Zamora, S., Stedmon, C., Nielsen, T.G., 2011. Phytoplankton growth and microzooplankton grazing along a sub-Arctic fjord (Godthåbsfjord, west Greenland). *Mar. Ecol. Prog. Ser.* 442, 11–22.
- Chu, V.W., 2014. Greenland ice sheet hydrology: a review. *Prog. Phys. Geogr.* 38, 19–54.
- Colas, F., Tardivel, M., Perchoc, J., Lunven, M., Forest, B., Guyader, G., Danielou, M.M., Mestre, S.L., Bourriau, P., Antajan, E., Sourisseau, M., Huret, M., Petitgas, P., Romagnan, J.B., 2018. The ZooCAM, a new in-flow imaging system for fast onboard counting, sizing and classification of fish eggs and metazooplankton. *Prog. Oceanogr.* 166, 54–65.
- Dalpadado, P., Hop, H., Rønning, J., Pavlov, V., Sperfeld, E., Buchholz, F., Rey, A., Wold, A., 2016. Distribution and abundance of euphausiids and pelagic amphipods in Kongsfjorden, Isfjorden and Rijpfjorden (Svalbard) and changes in their relative importance as key prey in a warming marine ecosystem. *Polar Biol.* 39, 1765–1784.
- Field, J.G., Clarke, K.R., Warwick, R.M., 1982. A practical strategy for analysing multi-species distribution patterns. *Mar. Ecol. Prog. Ser.* 8, 37–52.
- Gorsky, G., Ohman, M.D., Picheral, M., Gasparini, S., Stemann, L., Romagnan, J., Cawood, A., Pesant, S., García-Comas, C., Prejger, F., 2010. Digital zooplankton image analysis using the ZooScan integrated system. *J. Plankton Res.* 32, 285–303.
- Grosjean, P., Picheral, M., Warembourg, C., Gorsky, G., 2004. Enumeration, measurement, and identification of net zooplankton samples using the ZOOSCAN digital imaging system. *ICES J. Mar. Sci.* 61, 518–525.
- Herman, A.W., 1988. Simultaneous measurement of zooplankton and light attenuation with a new optical plankton counter. *Cont. Shelf Res.* 8, 205–221.
- Herman, A.W., 1992. Design and calibration of a new optical plankton counter capable of sizing small zooplankton. *Deep-Sea Res.* 39A, 395–415.
- Herman, A.W., Harvey, M., 2006. Application of normalized biomass size spectra to laser optical plankton counter net intercomparisons of zooplankton distributions. *J. Geophys. Res.* 111, C05S05. <https://doi.org/10.1029/2005JC002948>.
- Herz, L.E., 1933. The morphology of the later stages of *Balanus crenatus* Bruguier. *Biol. Bull.* 64, 432–442.
- Hop, H., Pearson, T., Hegseth, E.N., Kovacs, K.M., Wiencke, C., Kwasniewski, S., Eiane, K., Mehlum, F., Gulliksen, B., Włodarska-Kowalczyk, M., Lydersen, C., Weslawski, J.M., Cochrane, S., Gabrielsen, G.W., Leakey, R.J.G., Lønne, O.J., Zajaczkowski, M., Falk-Petersen, S., Kendall, M., Wängberg, S., Bischof, K., Voronkov, A.Y., Kovaltchouk, N.A., Wiktor, J., Poltermann, M., di Prisco, G., Papucci, C., Gerland, S., 2002. The marine ecosystem of Kongsfjorden, Svalbard. *Polar Res.* 21, 167–208.
- Howat, I.M., Eddy, A., 2011. Multi-decadal retreat of Greenland's marine-terminating glaciers. *J. Glaciol.* 57, 389–396.
- Kanna, N., Sugiyama, S., Ohashi, Y., Sakakibara, D., Fukamachi, Y., Nomura, D., 2018. Upwelling of macronutrients and dissolved inorganic carbon by a subglacial freshwater driven plume in Bowdoin Fjord, northwestern Greenland. *J. Geophys. Res. Biogeosci.* 123, 1666–1682.
- Lydersen, C., Assmy, P., Falk-Petersen, S., Kohler, J., Kovacs, K.M., Reigstad, M., Steen, H., Strøm, H., Sundfjord, A., Varpe, Ø., Walczowski, W., Weslawski, J.M., Zajaczkowski, M., 2014. The importance of tidewater glaciers for marine mammals and seabirds in Svalbard, Norway. *J. Mar. Syst.* 129, 452–471.
- Marcolin, C.R., Schultes, S., Jackson, G.A., Lopes, R.M., 2013. Plankton and seston size spectra estimated by the LOPC and ZooScan in the Abrolhos Bank ecosystem (SE Atlantic). *Cont. Shelf Res.* 70, 74–87.
- Marcolin, C.R., Gaeta, S., Lopes, R.M., 2015. Seasonal and interannual variability of zooplankton vertical distribution and biomass size spectra off Ubatuba, Brazil. *J. Plankton Res.* 37, 808–819.
- Matsuno, K., Yamaguchi, A., Imai, I., 2012. Biomass size spectra of mesozooplankton in the Chukchi Sea during the summers of 1991/1992 and 2007/2008: an analysis using optical plankton counter data. *ICES J. Mar. Sci.* 69, 1205–1217.
- Moore, S.K., Suthers, I.M., 2006. Evaluation and correction of subresolved particles by the optical plankton counter in three Australian estuaries with pristine to highly modified catchments. *J. Geophys. Res.* 111, C05S04.
- Motoda, S., 1959. Devices of simple plankton apparatus. *Mem. Fac. Fish. Hokkaido Univ.* 7, 73–94.
- Murray, T., Scharrer, K., Selmes, N., Booth, A.D., James, T.D., Bevan, S.L., Bradley, J., Cook, S., Cordero Llana, L., Drocourt, Y., Dyke, L., Goldsack, A., Hughes, A.L., Luckman, A.J., McGovern, J., 2015. Extensive retreat of Greenland tidewater glaciers, 2000–2010. *Arctic Antarct. Alpine Res.* 47, 427–447.
- Nishizawa, B., Kanna, N., Ohashi, Y., Sakakibara, D., Asaji, I., Abe, Y., Yamaguchi, A., Sugiyama, S., Watanuki, Y. Contrasting communities of seabirds in subglacial meltwater plume and oceanic water in Bowdoin fjord in northwestern Greenland. *ICES J. Mar. Sci.*, (submitted).
- Nogueira, E., González - Nuevo, G., Bode, A., Varela, M., Morán, X.A.G., Valdés, L., 2004. Comparison of biomass and size spectra derived from optical plankton counter data and net samples: application to the assessment of mesoplankton distribution along the Northwest and North Iberian Shelf. *ICES J. Mar. Sci.* 61, 508–517.
- Ohashi, Y., Iida, T., Sugiyama, S., Aoki, S., 2016. Spatial and temporal variations in high turbidity surface water off the Thule region, northwestern Greenland. *Pol. Sci.* 10, 270–277.
- Palma, S., Retamal, M.C., Silva, N., Silva, C., 2014. Horizontal and vertical distributions of siphonophores in relation to oceanographic conditions in Chilean Patagonian fjords. *Sci. Mar.* 78, 339–351.
- Riisgaard, K., Swalethorp, R., Kjellerup, S., Juul-Pedersen, T., Nielsen, T.G., 2014. Trophic role and top-down control of a subarctic protozooplankton community. *Mar. Ecol. Prog. Ser.* 500, 67–82.
- Sakakibara, D., Sugiyama, S., 2018. Ice front and flow speed variations of marine-terminating outlet glaciers along the coast of Prudhoe Land, northwestern Greenland. *J. Glaciol.* 64, 300–310.
- Schultes, S., Lopes, R.M., 2009. Laser Optical Plankton Counter and ZooScan inter-comparison in tropical and subtropical marine ecosystems. *Limnol. Oceanogr. Methods* 7, 771–784.
- Sprules, W.G., Munawar, M., 1986. Plankton size spectra in relation to ecosystem productivity, size, and perturbation. *Can. J. Fish. Aquat. Sci.* 43, 1789–1794.
- Sprules, W.G., Jin, E.H., Herman, A.W., Stockwell, J.D., 1998. Calibration of an optical plankton counter for use in fresh water. *Limnol. Oceanogr.* 43, 726–733.
- Sugiyama, S., Sakakibara, D., Tsutaki, S., Maruyama, M., Sawagaki, T., 2015. Glacier dynamics near the calving front of Bowdoin Glacier, northwestern Greenland. *J. Glaciol.* 61, 223–232.
- Swalethorp, R., Malanski, E., Agersted, M.D., Nielsen, T.G., Munk, P., 2015. Structuring of zooplankton and fish larvae assemblages in a freshwater-influenced Greenlandic fjord: influence from hydrography and prey availability. *J. Plankton Res.* 37, 102–119.
- Thompson, G.A., Dinofrio, E.O., Alender, V.A., 2013. Structure, abundance and biomass size spectra of copepods and other zooplankton communities in upper waters of the Southwestern Atlantic Ocean during summer. *J. Plankton Res.* 35, 610–629.
- Vandromme, P., Stemann, L., García-Comas, C., Berline, L., Sun, X., Gorsky, G., 2012. Assessing biases in computing size spectra of automatically classified zooplankton from imaging systems: a case study with the ZooScan integrated system. *Methods Oceanogr.* 1–2, 3–21.
- Vandromme, P., Nogueira, E., Huret, M., Lopez-Urrutia, Á., González-Nuevo González, G., Sourisseau, M., Petitgas, P., 2014. Springtime zooplankton size structure over the continental shelf of the Bay of Biscay. *Ocean Sci.* 10, 821–835.
- Yokoi, Y., Yamaguchi, A., Ikeda, T., 2008. Regional and interannual changes in the abundance, biomass and size structure of mesozooplankton in the western North Pacific in early summer analyzed using an optical plankton counter. *Bull. Plankton Soc. Jpn.* 55, 9–24 (in Japanese with English abstract).
- Zhang, X., Roman, M., Sanford, A., Adolf, H., Lascara, C., Burgett, R., 2000. Can an optical plankton counter produce reasonable estimates of zooplankton abundance and biovolume in water with high detritus? *J. Plankton Res.* 22, 137–150.
- Zhou, M., 2006. What determines the slope of a plankton biomass spectrum? *J. Plankton Res.* 28, 437–448.
- Zhou, M., Tande, K.S., Zhu, Y., Basedow, S., 2009. Productivity, trophic levels and size spectra of zooplankton in northern Norwegian shelf regions. *Deep-Sea Res.* II 56, 1934–1944.